

## Co-expression patterns of microglia markers Iba1, TMEM119 and P2RY12 in Alzheimer's disease

Boyd Kenkhuis <sup>a,b,\*</sup>, Antonios Somarakis <sup>b</sup>, Lynn R.T. Kleindouwel <sup>a,b</sup>, Willeke M. C. van Roon-Mom <sup>a</sup>, Thomas Höllt <sup>b,c</sup>, Louise van der Weerd <sup>a,b</sup>

<sup>a</sup> Department of Human Genetics, Leiden University Medical Center, Leiden, the Netherlands

<sup>b</sup> Department of Radiology, Leiden University Medical Center, Leiden, the Netherlands

<sup>c</sup> Department of Intelligent Systems, Delft University of Technology, Delft, the Netherlands

### ARTICLE INFO

#### Keywords:

Microglia  
Iba1  
TMEM119  
P2RY12  
Alzheimer's disease  
Immunohistochemistry

### ABSTRACT

Microglia have been identified as key players in Alzheimer's disease pathogenesis, and other neurodegenerative diseases. Iba1, and more specifically TMEM119 and P2RY12 are gaining ground as presumably more specific microglia markers, but comprehensive characterization of the expression of these three markers individually as well as combined is currently missing. Here we used a multispectral immunofluorescence dataset, in which over seventy thousand microglia from both aged controls and Alzheimer patients have been analysed for expression of Iba1, TMEM119 and P2RY12 on a single-cell level. For all markers, we studied the overlap and differences in expression patterns and the effect of proximity to  $\beta$ -amyloid plaques. We found no difference in absolute microglia numbers between control and Alzheimer subjects, but the prevalence of specific combinations of markers (phenotypes) differed greatly. In controls, the majority of microglia expressed all three markers. In Alzheimer patients, a significant loss of TMEM119<sup>+</sup>-phenotypes was observed, independent of the presence of  $\beta$ -amyloid plaques in its proximity. Contrary, phenotypes showing loss of P2RY12, but consistent Iba1 expression were increasingly prevalent around  $\beta$ -amyloid plaques. No morphological features were conclusively associated with loss or gain of any of the markers or any of the identified phenotypes. All in all, none of the three markers were expressed by all microglia, nor can be wholly regarded as a pan- or homeostatic marker, and preferential phenotypes were observed depending on the surrounding pathological or homeostatic environment. This work could help select and interpret microglia markers in previous and future studies.

### 1. Introduction

Microglia are the resident myeloid cells of the central nervous system, crucial for both development and homeostasis of the brain. With their highly motile processes, they continuously survey their microenvironment (Nimmerjahn et al., 2005), enabling them to not only act as first in line immune defense, but also help regulate brain activity (Badimon et al., 2020). Microglia are also implicated to play an important role in several neurodegenerative diseases, including Alzheimer's disease (AD) (Li and Barres, 2018). Genome wide association studies have identified many risk genes for AD, with the majority primarily or even exclusively expressed in microglia, indicative of a causal or augmentary role for microglia in disease pathogenesis (Jansen et al.,

2019). In line with this, transcriptomic studies have found microglia to show the most substantial changes in response to pathology in murine and human studies (Keren-Shaul et al., 2017; Krasemann et al., 2017; Zhou et al., 2020; Mathys et al., 2019). These studies highlight the importance of well-characterized tools to study microglia in both homeostasis and disease.

One of the most widely used techniques to study microglia is immunohistochemistry (IHC). For a long time, microglial researchers depended on classical myeloid cell markers, of which the most commonly used ones are ionized calcium binding adaptor molecule 1 (Iba1), MHCII cell surface receptor HLA-DR, CD11b and CD68. However, these markers do not allow distinguishing microglia from infiltrating macrophages. The importance of this distinction has become

**Abbreviations:** A $\beta$ , Amyloid- $\beta$ ; AD, Alzheimer's disease; CNS, Central Nervous System; Iba1, Ionized calcium binding adaptor molecule 1; IHC, Immunohistochemistry; TMEM119, Transmembrane protein 119.

\* Corresponding author at: Department of Human Genetics, Leiden University Medical Center, Albinusdreef 2, 2333 ZA Leiden, the Netherlands.

E-mail address: [b.kenkhuis@lumc.nl](mailto:b.kenkhuis@lumc.nl) (B. Kenkhuis).

<https://doi.org/10.1016/j.nbd.2022.105684>

Received 10 May 2021; Received in revised form 25 February 2022; Accepted 28 February 2022

Available online 2 March 2022

0969-9961/© 2022 The Authors. Published by Elsevier Inc. This is an open access article under the CC BY-NC-ND license (<http://creativecommons.org/licenses/by-nd/4.0/>).

increasingly clear, as microglia arise from embryonic yolk sac precursors during early embryonic development, which makes them ontogenically and transcriptionally distinct from blood-associated myeloid cells such as macrophages, that infiltrate the human CNS under pathological conditions (Ginhoux et al., 2010). Recently, researchers identified new genes that are almost exclusively expressed by microglia in CNS (Butovsky et al., 2014). The two most prominent examples of such genes are *TMEM119* and *P2RY12*, for which quickly novel antibodies were developed.

Transmembrane protein 119 (*TMEM119*), was characterized to be a specific microglia marker by Bennet et al. in 2016, although its function in microglia remains unknown (Bennett et al., 2016). It is considered to be a marker expressed by microglia under homeostatic conditions based on transcriptomic findings (Keren-Shaul et al., 2017; Krasemann et al., 2017; Butovsky et al., 2013). Also *in vitro* studies showed mRNA levels to be reduced when microglia are activated (Bennett et al., 2016). However, contrary to these results, increased mRNA levels have been found in AD brains (Jichi et al., 2016). *P2RY12* on the other hand, is a purinergic receptor that responds to ADP/ATP to increase cell migration. It was initially identified on platelets, and plays an important role in mediating platelet activation and blood clotting (Hollopeter et al., 2001). *P2RY12* was found to be exclusively expressed by microglia in the murine CNS (Butovsky et al., 2014), and is consistently expressed by human microglia throughout development (Mildner et al., 2017). Its expression is decreased under pathological conditions present in AD (Mildner et al., 2017), which Walker et al. later attributed to a specific lack of *P2RY12*-positive cells surrounding mature amyloid beta ( $A\beta$ ) plaques (Walker et al., 2020). However, *P2RY12* expression was also found on microglia positive for CD68 and HLA-DR, which are considered markers of activation (Walker et al., 2020). These findings suggest that *TMEM119* and *P2RY12* expression could encompass a wider range of microglia phenotypes than the originally hypothesized homeostatic subset.

While immunohistochemical evaluation of microglia using *TMEM119* and *P2RY12* is becoming more popular considering their microglia specificity, comprehensive data characterizing the expression in post-mortem AD brain tissue, as exists for the Iba1, CD68 and HLA-DR, is missing (Hopperton et al., 2018). Additionally, it is unknown what the overlap is between *TMEM119* and *P2RY12*, and the classical marker Iba1. Therefore, in this study we aimed to investigate the expression patterns of Iba1, *TMEM119* and *P2RY12* in AD and age-matched control tissue and more importantly the overlap and differences in expression patterns. To do so, we used a previously acquired multispectral immunofluorescence dataset published by Kenkhuis et al. (2021). On this dataset we performed a novel analysis using information about the expression of Iba1, *TMEM119* and *P2RY12* on a single-cell level and combined this with the spatial relationship with respect to  $A\beta$  plaques. We found a significant overall decrease of *TMEM119* positive microglia in AD patients, but a strong loss of *P2RY12* positivity and increase of Iba1 positivity specifically in  $A\beta$ -plaque surrounding microglia. Our findings highlight the differences in expression between these markers in response to pathology, and will help choose the appropriate microglia marker for future research.

## 2. Methods

### 2.1. Study design

This study was performed using the multispectral immunofluorescence dataset published by Kenkhuis et al. on brain autopsy tissue of the middle temporal gyrus of 12 AD patients and 9 age-matched non-neurological controls (Kenkhuis et al., 2021). Summary of group statistics can be found in Table 1 or individual patient characteristics can be found in Kenkhuis et al. One section per subject was stained for a combination of markers for nuclei (DAPI) microglia (*P2RY12*, *TMEM119* and Iba1) and  $A\beta$ -plaques. Subsequently all microglia were

**Table 1**  
Summary of patient statistics.

	Control (n = 9)	Alzheimer's disease (n = 12)	P-value
Age of onset, mean y (SD)	n.a	61.9 (16.9)	
Age of Death, mean y (SD)	82.3 (8.3)	74.8 (14.4)	0.1754
Male / female	4/5	3/9	0.3972
Braak stage, median (range)	1/2 (0–3)	6 (4–6)	< 0.0001
Thal Phase, median (range)	1 (0–2/3)	5 (3/4–5)	< 0.0001
Post-mortem interval, mean (SD)	6:56 (1:31)	4:49 (0:53)	0.001
APOE 2/3 - 3/3 - 3/4 - 4/4	0 - 3 - 1 - 0	1 - 5 - 4 - 2	

Difference in age of death and post-mortem interval was tested with a two-tailed Student's independent *t*-test, Braak stage and Thal phase with a Mann Whitney-U test and male / female distribution with a Fisher's exact test.

segmented and raw intensity fluorescence values for all intracellular markers were extracted. Additionally, all parenchymal  $A\beta$ -plaques were segmented and the distance of each identified microglia to a parenchymal plaque was reported. Finally, each identified microglia was also assigned a number, which can be traced back to the original image to evaluate marker expression and morphology manually.

### 2.2. Multispectral immunofluorescence

In short, 5- $\mu$ m-thick sections from Formalin fixed paraffin embedded (FFPE) tissue were deparaffinized with xylene and rehydrated using a gradient of 100%–50% alcohol. Endogenous peroxidases were blocked for 20 min in 0.3%  $H_2O_2$ /methanol and antigen-retrieval was performed by boiling the slides in pre-heated citrate (10 mM, pH = 6.0) for 10 min. Subsequently slides were blocked with blocking buffer (0.1% BSA/PBS + 0.05% Tween) for 30 min. Slides were then incubated sequentially with *TMEM119* (1:250, Sigma Aldrich; Overnight) and *P2RY12* (1:2500, Sigma Aldrich; 2 h), each of which were amplified firstly with Poly-HRP secondary antibody and secondly with an Opal tertiary antibody, before continuing to the next antibody. Subsequently, slides were incubated overnight with a cocktail of Ferritin Light-chain (1:100, Abcam),  $A\beta$  (1:250, Biolegend) and Iba1 (1:20, Millipore) antibodies, diluted in blocking buffer. The next day, slides were incubated with a secondary antibodies for G-a-riIgG A594, G-a-mIgG2b A647 and G-a-mIgG1 CF680 (1:200, ThermoFisher), diluted in 0.1% BSA/BPS. Finally, the slides were washed and incubated with 0.1  $\mu$ g/mL DAPI (Sigma Aldrich) for 5 min, after which they were mounted with 30  $\mu$ L Prolong diamond (ThermoFisher). A more extensive step-by-step protocol for the multispectral immunofluorescence panel can be found in Kenkhuis et al. (2021).

### 2.3. Data processing

Microglia were identified and segmented using a previously published inhouse cell segmentation pipeline (Kenkhuis et al., 2021). Raw fluorescence intensity values were normalized imposing Z-score transformation. To make our multispectral data comparable to traditional IHC studies, in which cells are usually scored as positive or negative for a certain marker, we aimed to set a threshold for positivity of an individual marker in our multispectral immunofluorescence data (Fig. 1A, B). Nevertheless, since the immunohistochemical signal is a continuum rather than binary output, it is important to note that cells that we rate as negative, can be positive for a specific marker, albeit it at lower levels than positive cells. We manually scored a subset of segmented microglia ( $n = 266$ ) for cell-positivity of *P2RY12*, *TMEM119* and Iba1, using a cell-positivity scoring scale (1: no signal; 2: sub-threshold positive, 3: positive signal, 4: very positive signal). Scoring was performed by two independent raters (BK and LRTK), after which a consensus score was reached (Supplementary Fig. 1A). By using the visually scored cells as

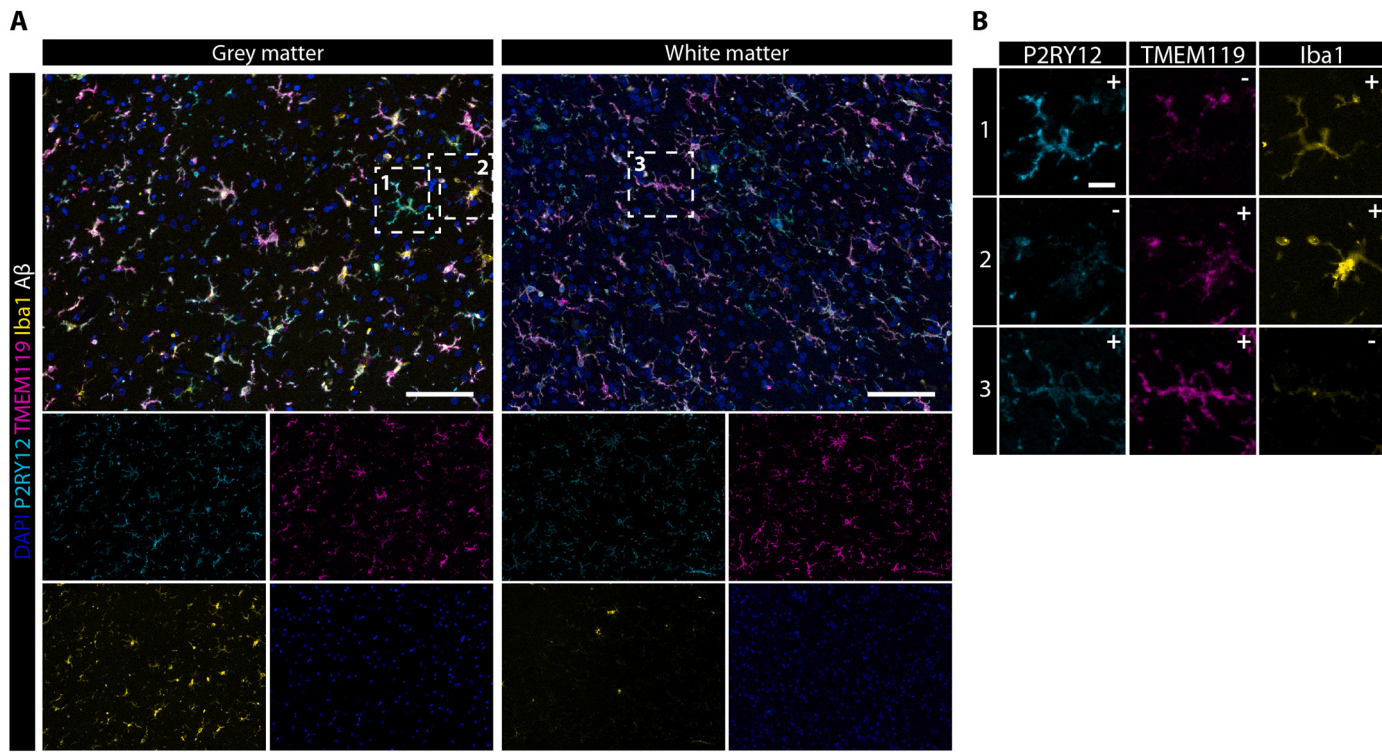


**Fig. 1.** Co-expression of P2RY12, TMEM119 and Iba1 in multispectral immunofluorescence data. *A* Example of multispectral data of grey- and white matter of a control subject. *B* Zooms of individual microglia cells with manual evaluation for positive expression of different markers. Scale bar, 100  $\mu$ m. Scale bar zoom, 20  $\mu$ m.

ground truth values, we determined the optimal threshold values by calculating which values yielded the greatest percentage of true positive and true negative cells (Supplementary Fig. 1B). The calculated threshold values lead to true positive and true negative percentages of respectively 91% and 90% for P2RY12, 83% and 84% for TMEM119 and 86% and 84% for Iba1. Based on these calculated threshold values, all microglia could be assessed for positivity of the individual markers, and clusters could be created based on the combination of expression of the different markers ( $P2RY12^{+/-}TMEM119^{-/+}Iba1^{-/+}$ ). As post-mortem interval differed significantly between controls and AD patients (Table 1), we interrogated the effect of post-mortem interval on staining parameters. As can be found in Supplementary Fig. 2A-B, no significant association was found between post-mortem interval and percentage of microglia positive for any of the markers.

#### 2.4. Statistical analysis

All variables were inspected for gaussian distribution of the data. Normally distributed data are represented by mean and standard deviation, whereas not normally distributed data are represented with the median and corresponding interquartile range, which is stated in the figure legend. Comparison of two continuous variables was performed using a two-tailed Student's independent *t*-test (normally distributed) or a Mann-Whitney *U* test (not normally distributed). Paired spatial data was analysed using a Repeated Measures ANOVA with Geisser-Greenhouse correction. Bonferroni post-hoc analysis was performed on individual analyses, and a significance level of  $P < 0.05$  was applied. All statistical tests were performed using GraphPad Prism (Version 8.00, La Jolla, San Diego, CA, USA).

### 3. Results

#### 3.1. Differing prevalence of phenotypes in control and AD patients

In total, 76.512 myeloid cells ( $n = 1419\text{--}6500$  per subject) were

identified in 21 subjects, which were positive for one or more of the microglia markers. No significant differences were observed in the total number of identified microglia between controls and AD patients, neither in the grey or white matter (Fig. 2A,B). Although the total number of microglia did not differ between control and AD tissue, we did observe differences in the expression of the individual markers between controls and AD patients. The percentage of  $TMEM119^{+}$ -microglia was significantly reduced in AD, both in the grey and in the white matter (Fig. 2C,D). For Iba1 and P2RY12 we did not observe significant differences, although  $P2RY12^{+}$ -microglia appeared to be less present in the grey matter AD patients (Fig. 2C). We also compared the percentage of positive microglia for each individual marker between grey and white matter, but did not find significant differences between the grey- and white matter cell populations. When looking at the raw fluorescent intensity of the different markers in positive cells, which is considered to be correlated with protein quantity, we found the mean intensity for P2RY12 and TMEM119 to be decreased in AD (Fig. 2E). We also studied whether combinations of these different markers ('phenotypes') were more or less present in AD (Fig. 2F). Interestingly, even though the overall percentage of  $Iba1^{+}$ -microglia was not increased in AD patients, microglia showing solely Iba1 expression without TMEM119 and P2RY12 (P4), were significantly more present in AD patients in both grey and white matter (Fig. 2G,H,I). Conversely,  $P2RY12^{+}TMEM119^{+}Iba1^{+}$ -microglia (P7) were significantly less prevalent in AD in the grey matter (Fig. 2G,H). In the white matter specifically,  $P2RY12^{-}$ - (P1) and  $P2RY12^{+}Iba1^{+}$ -microglia (P5) were more present in AD (Fig. 2I), though the observed effect of P1 was only borderline significant. Prevalence of phenotypes of all individual subjects that did not differ significantly can be found in Supplementary Fig. 3. These findings also show how the observed differences on single-marker level can be attributed to the combined differences in prevalence of the phenotypes. For both Iba1 and P2RY12, the increases observed in P1, P4 and P5 in AD are likely compensated by the decrease of P7 (Fig. 2H,I), resulting in no significant difference on single-marker level (Fig. 2C,D). For TMEM119 a significant decrease on single-marker levels

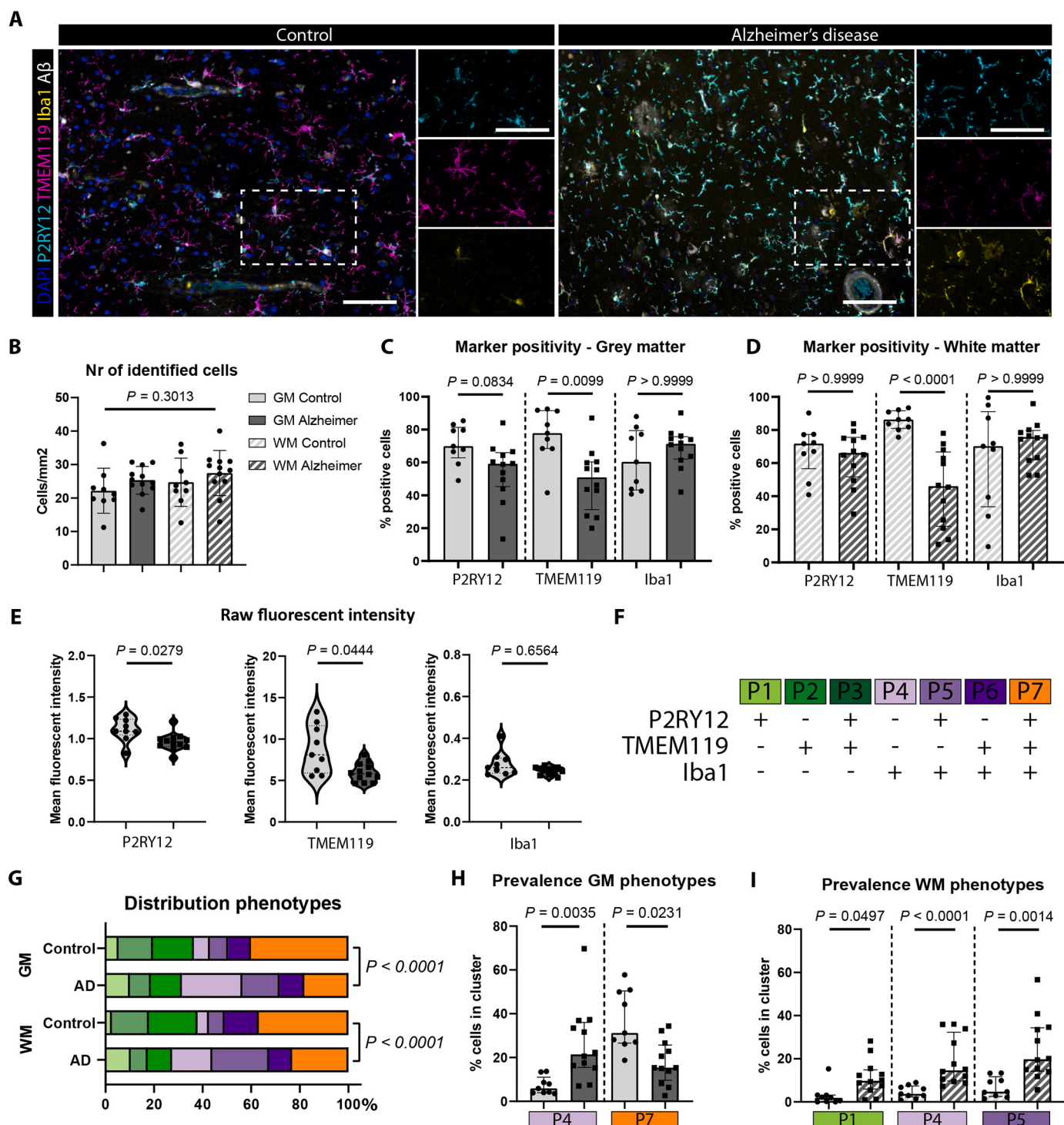


**Fig. 2.** Consistent loss of TMEM119<sup>+</sup>- and variable increase of P2RY12<sup>+</sup>/Iba1<sup>+</sup> phenotypes in Alzheimer brains. *A* Example image of control and AD patient with zooms showing individual markers. *B* Number of identified cells in the grey- and white matter of controls ( $n = 9$ ) and AD patients ( $n = 12$ ) (Mean, One-way Anova). Percentage of cells positive for the individual markers in grey matter (*C*) and white matter (*D*) (Median, Mann Whitney *U* test). *E* Mean fluorescent intensity of positive cells for P2RY12, TMEM119 and Iba1 (Median, Mann Whitney *U* test). *F* Created phenotypes (*P*) based on the combination of microglia markers present. *G* Distribution of identified phenotypes (*P1–P7*) in control and AD patients in the grey- and white matter differed significantly (Chi-square test). Additionally, prevalence of specific phenotypes differed significantly between control and AD patients for both the grey matter (GM) (*H*) and white matter (WM) (*I*) (Median, Mann-Whitney *U* test). *P*-values were corrected for multiple testing using Bonferroni within one graph (*C*, *D*, *E*, *H* and *I*). Scale bars, 100  $\mu$ m.

was found, which can be attributed to the consistent findings of TMEM119<sup>-</sup>-phenotypes to show increased prevalence (P1, P4, P5) and TMEM119<sup>+</sup>-phenotypes (P7) to show decreased prevalence in AD (Fig. 2H,I).

**3.2. *P2RY12*-expression but not *TMEM119* is negatively associated with A $\beta$ -plaques**

After analyzing the differences in expression of the microglia markers between control and AD patients, we investigated whether the

presence of A $\beta$ -plaques changed the expression patterns of our three microglia markers. First, we calculated the distance of all microglia with respect to A $\beta$ -plaques and divided them into three groups: infiltrating (0  $\mu$ m), surrounding (0–20  $\mu$ m) and no-plaque (>20  $\mu$ m) (Fig. 3A). Again, we first evaluated expression of the single microglial markers. Whereas the decrease in TMEM119 $^{+}$ -microglia in AD was again confirmed, no association with proximity to A $\beta$ -plaques was observed (Fig. 3B). Conversely, there was a significant reduction in the number of P2RY12 $^{+}$ -microglia infiltrating A $\beta$ -plaques in AD patients and an increase in the

cells positive for Iba1 in the plaque-surrounding microglia and even more so in the plaque-infiltrating microglia in both controls and AD patients (Fig. 3B). Next we investigated the effect of proximity to A $\beta$ -plaques on the previously defined phenotypes. In controls, there was a decrease of P1-P3 and increase of P4 and P7 for microglia getting closer to A $\beta$ -plaques (Fig. 3C). In AD patients, also a decrease in P1-P3 was observed. However, contrary to the controls, this was due to an increase of P4 and P6-microglia (Fig. 3C). This clearly indicates that the majority of A $\beta$ -plaque infiltrating microglia consistently express Iba1, but

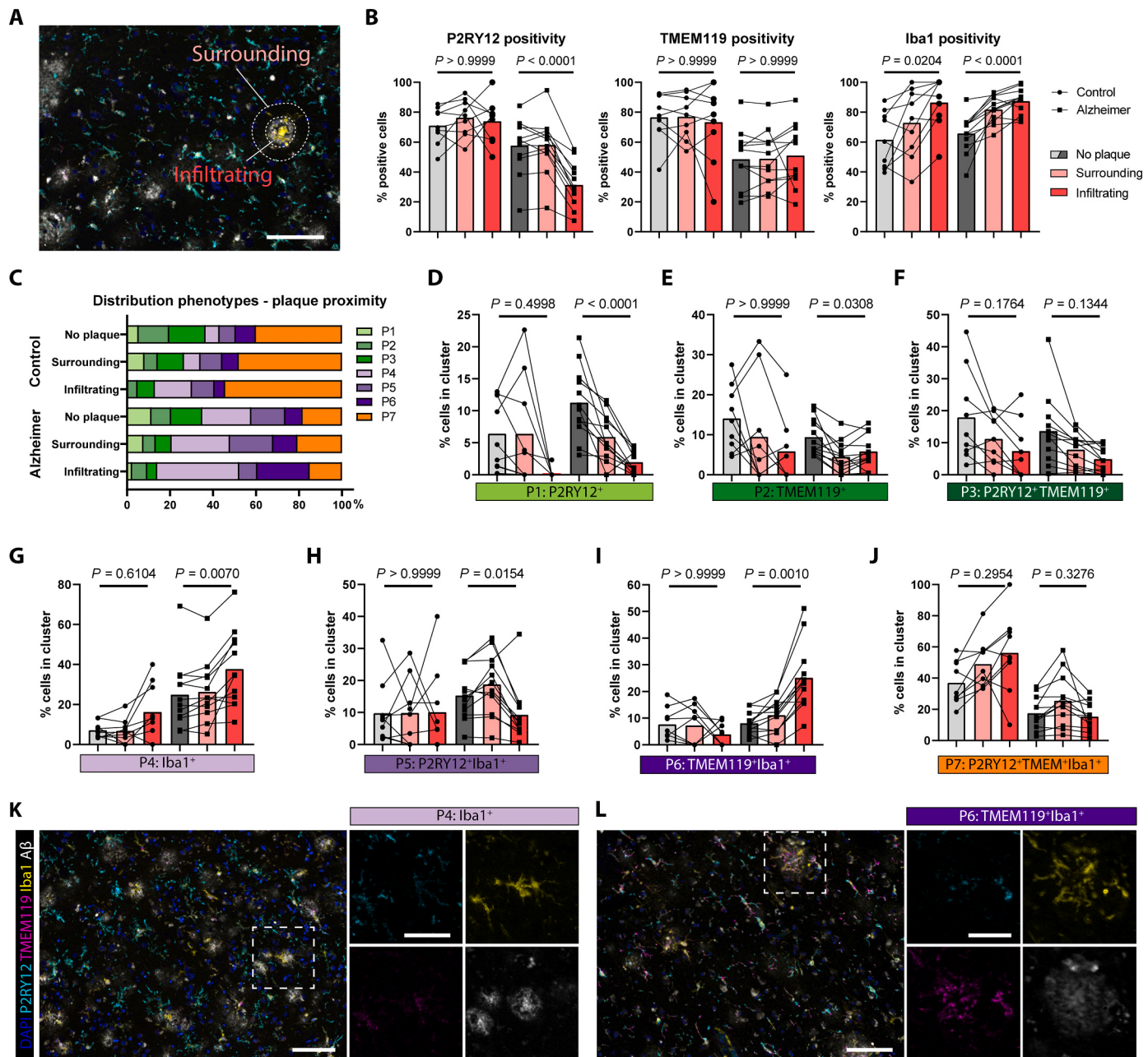


**Fig. 3.** Preferential A $\beta$ -plaque infiltration of Iba1 $^{+}$  and P2RY12 $^{-}$ -phenotypes in Alzheimer patients. **A** Example of how microglia are spatially subdivided into surrounding (Pink; 0 < x < 20  $\mu$ m), infiltrating (Red; 0  $\mu$ m) or no plaque (>20  $\mu$ m). **B** Prevalence of individual microglia markers in subdivided spatial groups of controls ( $n = 9$ ) and AD patients ( $n = 12$ ) (Mean). **C** Distribution of phenotypes P1-P7 subdivided in three groups based on A $\beta$  proximity. Comparison of the prevalence of different clusters based on proximity to A $\beta$ -plaques for cluster P1-P7 (D-J respectively). Example of infiltrating microglia of P4 (K) and P6 (L). For B and D-J, Stacked bars represent mean and statistical difference between spatial groups was tested using Repeated Measures ANOVA with Geisser-Greenhouse correction, individually for controls ( $n = 9$ ) and AD patients ( $n = 12$ ).  $P$ -values were corrected for multiple testing using Bonferroni for all test performed in B, and jointly on all test performed in D-J. Scale bars, 100  $\mu$ m. Scale bar zooms, 50  $\mu$ m. (For interpretation of the references to colour in this figure legend, the reader is referred to the web version of this article.)

variably show loss of TMEM119 and P2RY12. Subsequently we further looked into the observed trends in the individual subjects. None of the differences found in the control patients were found to be significant (Fig. 3D–J), which can be partially explained by the fact that fewer A $\beta$ -plaques are identified in control patients, and therefore the accuracy of the phenotype distribution is much lower. In AD patients, consistent patterns are observed within individuals. For the Iba1 $^{-}$ -phenotypes (P1–P3), P2RY12 $^{+}$ -microglia (P1) showed the most significant decrease in prevalence when getting closer to A $\beta$ -plaques (Fig. 3D–F). For the Iba1 $^{+}$ -phenotypes (P5–P7), both Iba1 $^{+}$ - (P4) and TMEM119 $^{+}$ Iba1 $^{+}$ -microglia (P6) showed significantly increased prevalence in microglia infiltrating A $\beta$ -plaques (Fig. 3G,I). Two examples of such phenotypes infiltrating microglia are shown in Fig. 3K and L respectively. Notably, even though

overall prevalence of Iba1 was increased for infiltrating microglia, P2RY12 $^{+}$ Iba1 $^{+}$ -microglia (P5) were significantly decreased in prevalence in A $\beta$ -plaque infiltrating microglia. All in all, the presence of A $\beta$ -plaques had the strongest effect on P2RY12-positivity, which was consistently decreased in plaque-infiltrating microglia (P1, P3, P5, P7). Most Iba1 $^{+}$ -phenotypes were increased (P4, P6), though not consistently for all Iba1 $^{+}$ -phenotypes (P5). No clear effect of the presence of A $\beta$ -plaques was observed on the percentage of TMEM119 $^{+}$ -microglia.

### 3.3. Morphology

Even though a large variety of activation-dependent microglia markers now exist, microglial morphology can add additional

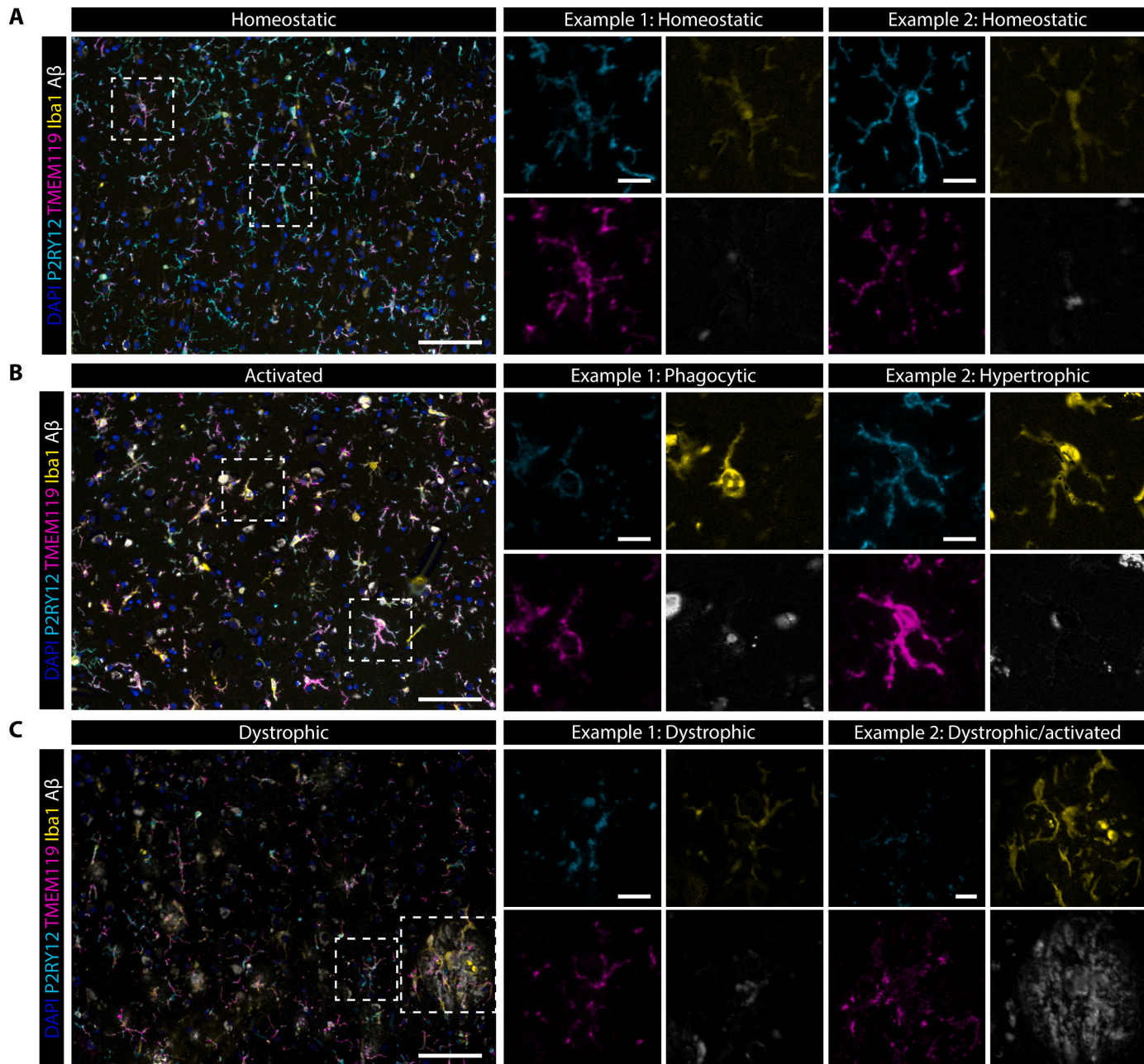


**Fig. 4.** Correlation of marker-expression with morphology. Representative images showing a general appearance of homeostatic (A), activated (B) and dystrophic (C) microglia, with zooms showing individual marker-expression of microglia of a specific subtype. Scale bars, 100  $\mu$ m. Scale bar zooms, 20  $\mu$ m.

information on microglial activation. Therefore we evaluated the relationship between expression of the P2RY12, TMEM119 and Iba1 with the classically defined morphological states: homeostatic, activated (which also encompasses phagocytic and rod-shaped), and dystrophic microglia (Streit et al., 2014). Morphological evaluation was performed by visually assessing 5–10 microglia per image, in a total of 130 images (3–8 images per subject), and comparing the morphologically evaluated microglia with P2RY12, TMEM119 and Iba1 expression.

Iba1-expression was identified on all three microglia morphological subtypes. However, noticeable is that even though the majority of homeostatic microglia showed positive Iba1 signal, the expression of Iba1 on activated microglia was generally higher (Fig. 4B vs. A). Dystrophic microglia only had higher Iba1 expression when there were signs of early dystrophy with spheroid formation, but enlarged soma were still visible. Once fragmentation of the branches occurred, usually Iba1 expression was also decreased (Fig. 4C-1). Finally, perivascular macrophages showed consistent high Iba1 expression.

Strong P2RY12 expression was consistently found on homeostatic microglia (Fig. 4A). Also both activated and dystrophic microglia generally still expressed P2RY12, though not as consistently as homeostatic (Fig. 4B-1). However, a clear exception to this consistent expression were microglia surrounding A $\beta$ -plaques (Fig. 4C), as described in the previous section. Apart from the spatial localization close to plaques, we did not observe clear morphological features associated with this specific plaque-related loss of P2RY12-expression.

TMEM119 was expressed on nearly all homeostatic microglia. Loss of TMEM119 was clearly found on a proportion of activated microglia, but not consistently across all (Fig. 4B-1 vs B-2). With regard to dystrophic microglia, a clear change in intracellular expression patterns was noticeable, with more punctate and irregular expression along the membrane, compared to homeostatic microglia. The clearest example of this disturbed distribution of TMEM119 was found in the A $\beta$ -plaque infiltrating microglia (Fig. 4C-2).

All in all, none of the markers showed a consistent change in expression by morphological subtype of microglia. TMEM119 and P2RY12 were both consistently found on homeostatic microglia, but showed variable expression on activated and dystrophic microglia, although no unique morphological features correlated with expression levels of any of the markers. These results indicate that although morphology can clearly depict whether cells have lost their homeostatic function, the morphological subtypes do not accurately reflect specific activation states resulting in loss or gain of any of the markers.

#### 4. Discussion

The present study is the first to quantify the co-expression patterns microglia specific markers TMEM119 and P2RY12, together with Iba1 in human control and AD brains. We found unique patterns for each of the markers, with a selective decrease of TMEM119 and P2RY12, and an increase of Iba1 in subsets in AD patients. Spatially, distinct phenotypes preferentially infiltrated A $\beta$ -plaques, and showed consistent Iba1 expression but marked loss of P2RY12, or both P2RY12 and TMEM119.

For Iba1, we found comparable numbers of positive cells in AD patients and controls, and it was consistently expressed in microglia surrounding and infiltrating A $\beta$ -plaques. This was in line with a systematic review, showing no significant increase in the number of identified Iba1-positive microglia in AD patients in the majority of studies (Hopperton et al., 2018). However, when using expression-based assays (IHC/western blot/qPCR) some studies did show a slight increase of Iba1-expression in microglia in AD (Hopperton et al., 2018; Ito et al., 1998). In our study, by visually evaluating different morphological subtypes, we found that activated microglia appeared to have higher expression of Iba1, though quantitative evaluation of all raw expression values showed no differences between controls and AD patients. Additionally, upon further stratification of the microglia based on A $\beta$ -plaque proximity, we did find a significant increase of the prevalence of Iba1 in

A $\beta$ -plaque surrounding and infiltrating microglia. Functionally, Iba1 is involved in the reorganization of the cell-skeleton by cross-linking actin to induce membrane ruffling (Sasaki et al., 2001), essential for both microglia motility and phagocytosis (Ohsawa et al., 2000). These are two principal features of activated microglia, potentially explaining the observed increase of Iba1 in the morphologically activated and A $\beta$ -plaque associated microglia in our study. Via co-staining for multiple markers we could verify that specific Iba1 $^{+}$ -microglia phenotypes are variably increased and decreased in AD, but do not result in an overall significant difference in prevalence as reported in the systematic review (Hopperton et al., 2018). Finally, even though Iba1 is often considered as a pan-marker for all microglia and macrophages (Hopperton et al., 2018; Streit et al., 2014; Walker and Lue, 2015; Zrzavy et al., 2017), we observed a significant amount of microglia that were Iba1 $^{-}$  (10–60%), especially in our controls. This discrepancy could be explained by the fact that studies with single Iba1 IHC or double-staining of Iba1 with P2RY12 or TMEM119 would have missed microglia solely expressing P2RY12 or TMEM119 (P1–2), resulting in a higher percentage of Iba1 $^{+}$  microglia. This had already been suggested by Hendricks et al., who qualitatively showed only scarce expression of Iba1 in ramified microglia in control tissue, and Iba1 not being expressed by all microglial activation stages (Hendrickx et al., 2017). Two other quantitative IHC studies using double stainings also described populations of microglia showing low Iba1 expression (Serrano-Pozo et al., 2013; Swanson et al., 2020). However, contrary to our results and that of Hendricks et al., they found these Iba1 $^{\text{low}}$  populations to be increased in AD. All in all, we can confirm quantitatively that Iba1 is not expressed on all microglia, though opposing literature exists on whether activated microglia shows increased or decreased expression.

Regarding P2RY12, in our study we did not find significant differences in the overall number of P2RY12 $^{+}$ -microglia. Nevertheless, specific phenotypes P2RY12 $^{+}$  phenotypes (P1 & P5) were found to be more prevalent, whereas others (P7) were less prevalent in AD. Correspondingly, a previous study by Swanson et al., showing the first quantification of P2RY12 expression in AD brains using single-cell histology analysis, also found no difference in the prevalence of microglia populations with high or low P2RY12 expression between controls and AD patients (Swanson et al., 2020). Further spatial investigation showed that P2RY12 $^{+}$ -phenotypes were specifically decreased in and surrounding A $\beta$ -plaques (P1 & P3), where P2RY12 $^{-}$ -phenotypes were more prevalent (P4, P6), which contributed to an overall loss of P2RY12 microglia infiltrating A $\beta$ -plaques. These findings confirm previous observations of areas lacking P2RY12 $^{+}$ -microglia around A $\beta$ -plaques in AD patients (Mildner et al., 2017; Walker et al., 2020). Functionally, it was found that the P2Y12-receptor can induce microglial chemotaxis after binding of ligands such as ATP/ADP or extracellular nucleotides (Davalos et al., 2005; Haynes et al., 2006). This indicates P2RY12 to play an important role during early stages of microglia activation in response to CNS injury or blood-brain barrier damage (Haynes et al., 2006; Lou et al., 2016), after which expression is lost. *In vitro* results are in line with this, showing P2RY12 downregulation after activation with LPS (Van Wageningen et al., 2019; Banerjee et al., 2020). Also for multiple sclerosis this pattern is observed, with general decrease of P2RY12 expression, and almost complete loss in white matter lesions (Mildner et al., 2017; Zrzavy et al., 2017; Van Wageningen et al., 2019). Interestingly, in our human post-mortem AD tissue, P2RY12 was still variably expressed throughout the brain by microglia with both activated or dystrophic morphological appearance, but only specifically lost surrounding A $\beta$ -plaques. From this one can conclude that although P2RY12 appears to be a protein predominantly expressed in homeostatic microglia, its expression is only lost under very specific conditions, and presence of P2RY12 does not conclusively indicate a homeostatic function.

Lastly, a significant reduction of TMEM119 $^{+}$ -microglia and expression levels was found in AD. Interestingly, in contrast to P2RY12, this was generally not associated with A $\beta$ -plaques. Though one subset of microglia which was significantly associated with A $\beta$ -plaques showed

loss of both TMEM119 and P2RY12-expression (P5), another A $\beta$ -associated subset still expressed TMEM119 (P7). The majority of changes regarding A $\beta$ -associated TMEM119 expression can likely be attributed to the fact that we used relative numbers. To illustrate, an increase of TMEM119 $^+Iba1^+$  (P6) microglia could be observed due to loss of P2RY12 by TMEM119 $^+Iba1^+P2RY12^+$  microglia, instead of a change of TMEM119 expression. A $\beta$ -induced expression of TMEM119 seems unlikely considering overall TMEM119 expression was not affected by A $\beta$  plaque proximity in any of the subjects (Fig. 3B). Notably, even though TMEM119 was still expressed in a subset of microglia infiltrating A $\beta$  plaques, the protein appeared to be redistributed and did not show a homogenous appearance along the membrane as observed in controls patients. To date, only few have studied the expression of TMEM119 in microglia in aged and AD patients. Firstly, in line with our results, Swanson et al found a significant increase of a microglia population with low TMEM119 expression in AD patients. Secondly, using RT-PCR, an increase of TMEM119 mRNA was observed in AD brains, though this could not be confirmed on western blot (Jichi et al., 2016). In other diseases such as multiple sclerosis, researchers found a significant decrease in white matter lesions (Jichi et al., 2016; Van Wageningen et al., 2019), but a different study interpreted this as the cells being macrophages (Zrzavy et al., 2017). Additionally, very little is known about the function of TMEM119 in microglia. Consequently, TMEM119 is still occasionally incorrectly considered to be consistently expressed by microglia under both homeostatic and disease conditions, and used to discriminate microglia from blood-derived macrophages. However, our results indicate that TMEM119 expression is also dependent on activation state; its expression is decreased in an activated, though partially disparate subset than P2RY12 $^-$ -microglia. Cells lacking TMEM119 expression but with clear Iba1 and or P2RY12 expression were consistently observed in the parenchyma and showed clear microglia morphology. This indicates that a lack of expression of TMEM119 on an Iba1-positive cell does not necessarily indicate that the observed cell is not of microglial origin.

All in all, this work aids to the body of literature available on immunohistochemical markers used for microglia research. By employing multispectral immunofluorescence to specifically study the co-expression patterns of these microglia markers enabled us to show the overlap and differences in expression in control aged and diseased

brains, and in relation to A $\beta$ -plaques. This manuscript can therefore serve as a reference, but cannot help elucidate how A $\beta$  plaques mechanistically affects expression of these markers. As we aimed to help researchers interpret their immunohistochemical studies, we analysed the expression patterns as being either positive or negative for a marker. However, given the high-dimensional nature of the data (single-cell protein measures of 76.512 cells), also more novel visualization techniques such as t-distributed stochastic neighbor embedding (t-SNE) can be applied, and have been shown by Kenkhuis et al. (2021). Finally thanks to the automated microglia identification and marker evaluation, this work could easily be extended in the future with more recently identified microglia markers such as Hexb and Siglec-H (Konishi et al., 2017; Masuda et al., 2020).

## 5. Conclusion

This work helps interpret previous and future studies using Iba1, TMEM119 and P2RY12 or a combination of these markers. Therefore, we have created a figure (Fig. 5) to briefly summarize specific findings about Iba1, TMEM119 and P2RY12 expression, which can help interpret one's own study. The occurrence of different combinations of markers appeared heterogeneous, likely reflecting the myriad of functions microglia execute, and not general morphological activation states. Additionally, based on this study one can conclude that when evaluating microglia numbers, it is important to always stain for multiple different microglia markers, as none of the markers are expressed by all microglia, and an observed difference in microglia numbers could be due to a loss of marker expression, rather than loss of microglia. The same applies when studying macrophage-infiltration, as lack of TMEM119 does not immediately indicate macrophage rather than microglial origin.

## Ethics approval and consent to participate

All material has been collected with written consent from the donors and the procedures have been approved by the Medical Ethical committee of the LUMC and the Amsterdam UMC.

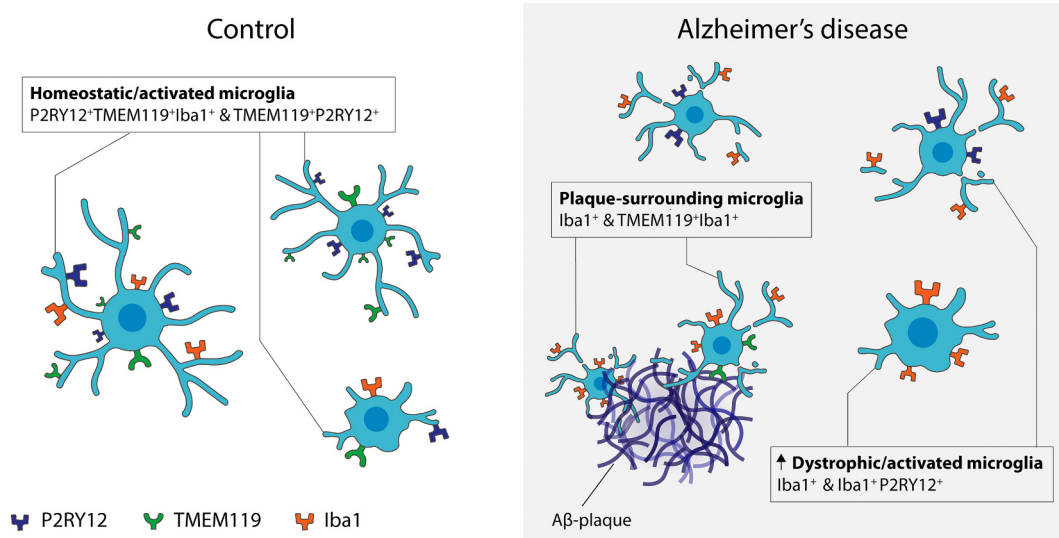


**Fig. 5.** Schematic of observed findings in control and AD patients. In controls the majority of microglia express all three markers or TMEM119 and P2RY12. On the other hand, microglia solely expressing Iba1 are more present in AD patients, as are microglia expressing Iba1 with either TMEM119 or P2RY12. These results indicate a shift from microglia with predominant TMEM119/P2RY12 expression to a microglia state with more Iba1 expression and loss of TMEM119 and/or P2RY12 in AD patients. Loss of P2RY12 was specifically attributed to presence of A $\beta$ -plaques, whereas TMEM119 was more generally lost in both grey and white matter.

## Consent for publication

Not applicable.

## Funding

B.K. is supported by an MD/PhD-grant from the Leiden University Medical Center. In addition, he has received funding from an early career fellowship from Alzheimer Nederland (WE.15-2018-13) and a Eurolife Scholarship for Early Career researchers. A.S. has received funding through Leiden University Data Science Research Programme. LvdW received funding from The Netherlands Organization for Scientific Research (NWO) Innovational Research Incentives Scheme (VIDI 864.13.014).

## Data availability

Data sharing is not applicable to this article as no datasets were generated. Scripts for data analysis are available from the corresponding author upon reasonable request.

## Authors' contributions

B.K. and L.v.d.W. conceived and designed the project. B.K. acquired the multispectral immunofluorescence (mIF) data. A.S. and B.K. created the microglia segmentation pipeline. B.K. and L.R.T.K. assessed data-quality and manually scored subsets of data. A.S. created the spatial analysis tools for mIF data under supervision of T.H. B.K performed morphological evaluation of microglia. B.K. and A.S. analysed and interpreted the mIF data. B.K., W.M.C.v.R-M, and L.v.d.W. wrote the manuscript. All authors read and approved the final manuscript.

## Declaration of Competing Interest

The authors have no conflicts of interest to declare. All co-authors have seen and agree with the contents of the manuscript and there is no financial interest to report.

## Acknowledgements

We acknowledge all patients who donated their brain to the Leiden University Medical Center (LUMC), Netherlands Brain Bank (NBB) or the Normal Aging Brain collection Amsterdam (NABCA), and prof. A.J. M. Rozemuller for neuropathological evaluation of the brains. We would like to thank the department of Pathology of the LUMC, especially Marieke IJsselsteijn and Noel de Miranda for their help with setting up multispectral immunofluorescence for microglia. We owe thanks to O. Dzyubachyk, B.P.F. Lelieveldt and J. Dijkstra for support in the analysis of the multispectral immunofluorescence data.

## Appendix A. Supplementary data

Supplementary data to this article can be found online at <https://doi.org/10.1016/j.nbd.2022.105684>.

## References

- Badimon, A., Strasburger, H.J., Ayata, P., Chen, X., Nair, A., Ikegami, A., et al., 2020. Negative feedback control of neuronal activity by microglia. *Nature* 586 (7829), 417–423.
- Banerjee, P., Paza, E., Perkins, E.M., James, O.G., Kenkhuis, B., Lloyd, A.F., et al., 2020. Generation of pure monocultures of human microglia-like cells from induced pluripotent stem cells. *Stem Cell Res.* 49.
- Bennett, M.L., Bennett, F.C., Liddelow, S.A., Ajami, B., Zamanian, J.L., Fernhoff, N.B., et al., 2016. New tools for studying microglia in the mouse and human CNS. *Proc. Natl. Acad. Sci. U. S. A.* 113 (12), E1738–E1746.
- Butovsky, O., Jedrychowski, M.P., Moore, C.S., Cialic, R., Lanser, A.J., Gabrely, G., et al., 2013. Identification of a unique TGF- $\beta$ -dependent molecular and functional signature in microglia. *Nat. Neurosci.* 17 (1), 131–143.
- Butovsky, O., Jedrychowski, M.P., Moore, C.S., Cialic, R., Lanser, A.J., Gabrely, G., et al., 2014. Identification of a unique TGF- $\beta$ -dependent molecular and functional signature in microglia. *Nat. Neurosci.* 17 (1), 131–143.
- Davalos, D., Grutzendler, J., Yang, G., Kim, J.V., Zuo, Y., Jung, S., et al., 2005. ATP mediates rapid microglial response to local brain injury in vivo. *Nat. Neurosci.* 8 (6), 752–758.
- Ginhoux, F., Greter, M., Leboeuf, M., Nandi, S., See, P., Gokhan, S., et al., 2010. Fate mapping analysis reveals that adult microglia derive from primitive macrophages. *Science* (80- (6005), 841–845.
- Haynes, S.E., Hollopeter, G., Yang, G., Kurpius, D., Dailey, M.E., Gan, W.B., et al., 2006. The P2Y12 receptor regulates microglial activation by extracellular nucleotides. *Nat. Neurosci.* 9 (12), 1512–1519.
- Herrick, D.A.E., van Eden, C.G., Schuurman, K.G., Hamann, J., Huitinga, I., 2017. Staining of HLA-DR, Iba1 and CD68 in human microglia reveals partially overlapping expression depending on cellular morphology and pathology. *J. Neuroimmunol.* 309, 12–22.
- Hollopeter, G., Jantzen, H.M., Vincent, D., Li, G., England, L., Ramakrishnan, V., et al., 2001. Identification of the platelet ADP receptor targeted by antithrombotic drugs. *Nature* 409 (6817), 202–207.
- Hoppert, K.E., Mohammad, D., Trépanier, M.O., Giuliano, V., Bazinet, R.P., 2018. Markers of microglia in post-mortem brain samples from patients with Alzheimer's disease: a systematic review. *Mol. Psychiatry* 23, 177–198.
- Ito, D., Imai, Y., Ohsawa, K., Nakajima, K., Fukuchi, Y., Kohsaka, S., 1998. Microglia-specific localisation of a novel calcium binding protein, Iba1. *Mol. Brain Res.* 57 (17), 1–9.
- Jansen, I.E., Savage, J.E., Watanabe, K., Bryois, J., Williams, D.M., Steinberg, S., et al., 2019. Genome-wide meta-analysis identifies new loci and functional pathways influencing Alzheimer's disease risk. *Nat. Genet.* 51 (3), 404–413.
- Jichi, Satoh, Kino, Y., Asahina, N., Takitani, M., Miyoshi, J., Ishida, T., et al., 2016. TMEM119 marks a subset of microglia in the human brain. *Neuropathology* 36 (1), 39–49.
- Kenkhuis, B., Somarakis, A., de Haan, L., Dzyubachyk, O., Ijsselsteijn, M.E., de Miranda, N., et al., 2021. Iron loading is a prominent feature of activated microglia in Alzheimer's disease patients. *Acta Neuropathol. Commun.* 9 (1), 27.
- Keren-Shaul, H., Spivrad, A., Weiner, A., Matcovitch-Natan, O., Dvir-Szternfeld, R., Ulland, T.K., et al., 2017. A unique microglia type associated with restricting development of Alzheimer's disease. *Cell* 169 (7), 1276–1290.e17.
- Konishi, H., Kobayashi, M., Kunisawa, T., Imai, K., Sayo, A., Malissen, B., et al., 2017. Siglec-H is a microglia-specific marker that discriminates microglia from CNS-associated macrophages and CNS-infiltrating monocytes. *Glia* 65 (12), 1927–1943.
- Krasemann, S., Madore, C., Cialic, R., Baufeld, C., Calcagno, N., El Fatimy, R., et al., 2017. The TREM2-APOE pathway drives the transcriptional phenotype of dysfunctional microglia in neurodegenerative diseases. *Immunity* 47 (3), 566–581.e9.
- Li, Q., Barres, B.A., 2018. Microglia and macrophages in brain homeostasis and disease. *Nat. Rev. Immunol.* 18, 225–242.
- Lou, N., Takano, T., Pei, Y., Xavier, A.L., Goldman, S.A., Nedergaard, M., 2016. Purinergic receptor P2RY12-dependent microglial closure of the injured blood-brain barrier. *Proc. Natl. Acad. Sci. U. S. A.* 113 (4), 1074–1079.
- Masuda, T., Amann, L., Sankowski, R., Staszewski, O., Lenz, M., D'Errico, P., et al., 2020. Novel Hexb-based tools for studying microglia in the CNS. *Nat. Immunol.* 21 (7), 802–815.
- Mathys, H., Davila-Velderrain, J., Peng, Z., Gao, F., Mohammadi, S., Young, J.Z., et al., 2019. Single-cell transcriptomic analysis of Alzheimer's disease. *Nature* 1.
- Mildner, A., Huang, H., Radke, J., Stenzel, W., Priller, J., 2017. P2Y 12 receptor is expressed on human microglia under physiological conditions throughout development and is sensitive to neuroinflammatory diseases. *Glia* 65 (2), 375–387.
- Nimmerjahn, A., Kirchhoff, F., Helmchen, F., 2005. Neuroscience: resting microglial cells are highly dynamic surveillants of brain parenchyma in vivo. *Science* (80- (308 (5726)), 1314–1318.
- Ohsawa, K., Imai, Y., Kanazawa, H., Sasaki, Y., Kohsaka, S., 2000. Involvement of Iba1 in membrane ruffling and phagocytosis of macrophages/microglia. *J. Cell Sci.* 113 (17), 3073–3084.
- Sasaki, Y., Ohsawa, K., Kanazawa, H., Kohsaka, S., Imai, Y., 2001. Iba1 is an actin-cross-linking protein in macrophages/microglia. *Biochem. Biophys. Res. Commun.* 286 (2), 292–297.
- Serrano-Pozo, A., Gómez-Isla, T., Growdon, J.H., Frosch, M.P., Hyman, B.T., 2013. A phenotypic change but not proliferation underlies glial responses in Alzheimer disease. *Am. J. Pathol.* 182 (6), 2332–2344.
- Streit, W.J., Xue, Q.S., Tischer, J., Bechmann, I., 2014. Microglial pathology. *Acta Neuropathol. Commun.* 2 (1), 1–17.
- Swanson, M.E.V., Scotter, E.L., Smyth, L.C.D., Murray, H.C., Ryan, B., Turner, C., et al., 2020. Identification of a dysfunctional microglial population in human Alzheimer's disease cortex using novel single-cell histology image analysis. *Acta Neuropathol. Commun.* 8 (1), 170.
- Van Wageningen, T.A., Vlaar, E., Kooij, G., Jongenelen, C.A.M., Geurts, J.J.G., 2019. Van dam AM. Regulation of microglial TMEM119 and P2RY12 immunoreactivity in multiple sclerosis white and grey matter lesions is dependent on their inflammatory environment. *Acta Neuropathol. Commun.* 7 (1).

- Walker, D.G., Lue, L.-F., 2015. Immune phenotypes of microglia in human neurodegenerative disease: challenges to detecting microglial polarization in human brains. *Alzheimers Res. Ther.* 7 (1), 56.
- Walker, D.G., Tang, T.M., Mendaikhan, A., Tooyama, I., Serrano, G.E., Sue, L.I., et al., 2020. Patterns of expression of purinergic receptor P2RY12, a putative marker for non-activated microglia, in aged and alzheimer's disease brains. *Int. J. Mol. Sci.* 21 (2).
- Zhou, Y., Song, W.M., Andhey, P.S., Swain, A., Levy, T., Miller, K.R., et al., 2020. Human and mouse single-nucleus transcriptomics reveal TREM2-dependent and TREM2-independent cellular responses in Alzheimer's disease. *Nat. Med.* 26 (1), 131–142.
- Zravy, T., Hametner, S., Wimmer, I., Butovsky, O., Weiner, H.L., Lassmann, H., 2017. Loss of "homeostatic" microglia and patterns of their activation in active multiple sclerosis. *Brain* 140 (7), 1900–1913.